7-Carboxy-7-deazaguanine Synthase: A Radical

JACS
JOURNAL OF THE AMERICAN CHEMICAL SOCIETY
Article
pubs.acs.org/JACS

7-Carboxy-7-deazaguanine Synthase: A Radical *S*-Adenosyl-L-methionine Enzyme with Polar Tendencies

Nathan A. Bruender,[†,¶] Tsehai A. J. Grell,[‡] Daniel P. Dowling,[‡,§,▽] Reid M. McCarty,[∥,#] Catherine L. Drennan,[‡,§,⊥] and Vahe Bandarian*[,†]

[†]Department of Chemistry, University of Utah, Salt Lake City, Utah 84112, United States
[‡]Department of Chemistry and [§]Howard Hughes Medical Institute and [⊥]Department of Biology, Massachusetts Institute of Technology, Cambridge, Massachusetts 02139, United States
[∥]Department of Chemistry and Biochemistry, University of Arizona, Tucson, Arizona 85721, United States

Supporting Information

ABSTRACT: Radical *S*-adenosyl-L-methionine (SAM) enzymes are widely distributed and catalyze diverse reactions. SAM binds to the unique iron atom of a site-differentiated [4Fe-4S] cluster and is reductively cleaved to generate a 5′-deoxyadenosyl radical, which initiates turnover. 7-Carboxy-7-deazaguanine (CDG) synthase (QueE) catalyzes a key step in the biosynthesis of 7-deazapurine containing natural products. 6-Carboxypterin (6-CP), an oxidized analogue of the natural substrate 6-carboxy-5,6,7,8-tetrahydropterin (CPH_4), is shown to be an alternate substrate for CDG synthase. Under reducing conditions that would promote the reductive cleavage of SAM, 6-CP is turned over to 6-deoxyadenosylpterin (6-dAP), presumably by radical addition of the 5′-deoxyadenosine followed by oxidative decarboxylation to the product. By contrast, in the absence of the strong reductant, dithionite, the carboxylate of 6-CP is esterified to generate 6-carboxypterin-5′-deoxyadenosyl ester (6-CP-dAdo ester). Structural studies with 6-CP and SAM also reveal electron density consistent with the ester product being formed in crystallo. The differential reactivity of 6-CP under reducing and nonreducing conditions highlights the ability of radical SAM enzymes to carry out both polar and radical transformations in the same active site.

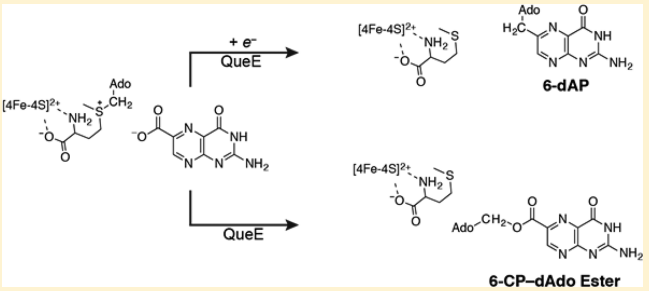

INTRODUCTION

The radical *S*-adenosyl-L-methionine (SAM) superfamily is a group of enzymes that harness the reductive cleavage of SAM to carry out complex radical-mediated transformations.[1] The superfamily was initially identified on the basis of a conserved CxxxCxxC motif,[2] which binds a site-differentiated [4Fe-4S] cluster whereby the three cysteine-thiolates coordinate the cluster. The fourth iron interacts with the α-amino and α-carboxylate of SAM.[3,4] To date, with only a few notable exceptions, the mechanisms of action for all radical SAM enzymes that have been proposed involve radical-mediated transformations that are initiated by the 5′-deoxyadenosyl radical (dAdo·), which is generated from the reductive cleavage of SAM (Figure 1A). The exception to this is the enzyme Dph2 involved in diphthamide biosynthesis, which generates a 3-amino-3-carboxypropyl radical.[5] The RNA methylases RlmN and Cfr consume two equivalents of SAM catalyzing both polar and radical-mediated group transfer reactions in the same catalytic cycle.[6,7] The first equivalent of SAM methylates an active site Cys releasing *S*-adenosylhomocysteine. Binding and reductive cleavage of the second equivalent of SAM initiates the radical-mediated transfer of the methyl group from the active site methyl-Cys residue to either the C2- or C8-position of A_{2503} in 23S rRNA. Finally, the cobalamin-dependent radical SAM enzyme TsrM catalyzes the methylation at C8 of the indole on tryptophan using a SAM-derived methyl group. The mechanism of this reaction remains to be established, but formation of 5′-deoxyadenosine (5′-dAdo) is not observed in this transformation.[8−10]

Recent bioinformatic analysis of the radical SAM superfamily has revealed >113 000 homologues in genome sequences, nearly all of which are enzymes that have been placed in this superfamily on the basis of the presence of the conserved CxxxCxxC sequence.[2,11] However, the ability of RlmN, Cfr, or TsrM to carry out both polar and/or radical transformations suggests that the conserved sequence motif may not ideally describe the expected range of reactivity. Perhaps some of the putative radical SAM proteins could utilize the activated sulfonium in SAM to catalyze polar group transfer chemistry. If true, it is likely that nonreductive group transfer chemistry may be an as yet uncharacterized promiscuous activity in radical SAM enzymes.

Received: November 2, 2016
Published: January 3, 2017

DOI: 10.1021/jacs.6b11381
J. Am. Chem. Soc. 2017, 139, 1912−1920

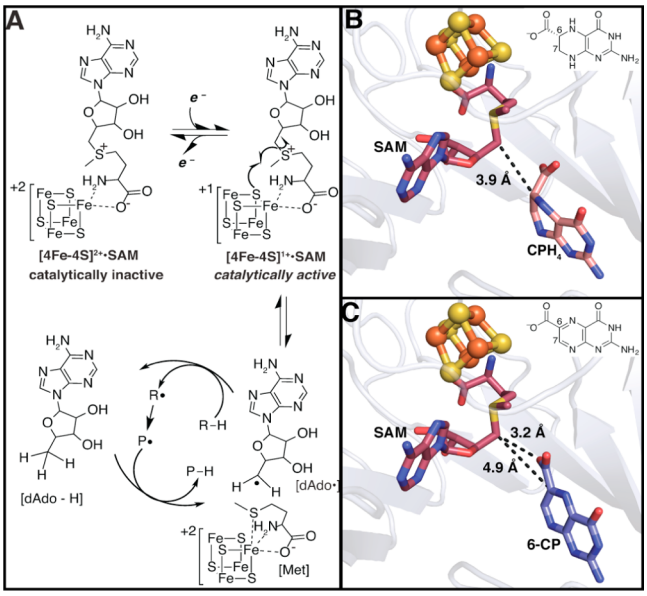

Figure 1. Schematic of radical SAM chemistry and active site view for the ligand complexes of *Burkholderia multivorans* QueE. (A) The [4Fe-4S] cluster of a radical SAM enzyme is reduced from the +2 to the +1 oxidation state by an electron from an external source. In vitro, electrons are commonly supplied from NADPH via the biological reducing system Fpr/Fld or from chemical reductants such as dithionite. SAM is reductively cleaved to form dAdo· and L-methionine upon inner sphere electron transfer from the [4Fe-4S] cluster to the sulfonium of SAM. dAdo· abstracts a H atom from the substrate to initiate the catalytic cycle. Some radical SAM enzymes reform the cofactor at the end of the catalytic cycle. (B) For *Bm*QueE, the 5′-carbon of the deoxyadenosine moiety of SAM (maroon) is 3.9 Å from the C-6 carbon of the substrate CPH_4 (salmon) (PDB 4NJI). The [4Fe-4S] cluster is displayed as yellow and orange spheres. Nitrogen atoms are in blue, oxygen are in red, and sulfur are in yellow. (C) The 5′-carbon of the deoxyadenosine moiety of SAM (maroon) is 3.2 and 4.9 Å from a carboxylate oxygen and the C-6 of 6-CP (gray), respectively (PDB 4NJG).

7-Carboxy-7-deazaguanine (CDG) synthase (QueE) is a member of the radical SAM superfamily that catalyzes the radical-mediated ring rearrangement required to convert 6-carboxy-5,6,7,8-tetrahydropterin (CPH_4) into CDG, which is the precursor to all pyrrolopyrimidine metabolites observed in nature.[12,13] Prior investigations have shown that QueE contains one [4Fe-4S] cluster that mediates the reductive cleavage of SAM (Figure 1A).[14,15] Reducing equivalents can be supplied in vitro from NADPH via ferredoxin(flavodoxin):$NADP^+$ reductase (Fpr) and flavodoxin (Fld) or via the chemical reductant dithionite.[14−16] Once formed, the dAdo· abstracts the C6 hydrogen atom from the substrate to initiate the ring rearrangement and subsequent elimination of N5 from the pterin.[14]

Recent X-ray crystal structures of the QueE homologue from *Burkholderia multivorans* (*Bm*QueE) in complex with SAM and substrate (CPH_4), product (CDG), or the substrate analogue 6-carboxypterin (6-CP), have provided invaluable snapshots of the active site of the protein (Figure 1B, Figure S1).[15] The overall structure of the *Bm*QueE is similar to other radical SAM enzymes,[17,18] with a few exceptions including an 11-residue insertion in the radical SAM cysteine motif that forms a 3_{10}-helix at the surface of the protein. The CPH_4-bound structure of QueE shows that the 5′-position of SAM is within 3.9 Å of C-6 of the substrate, which biochemical studies have shown to be the site of the H atom abstracted by the dAdo· to initiate catalysis (Figure 1B).[14,15] These observations are complemented by spectroscopic studies in other systems that suggest the role of radical SAM enzymes is to generate and shield/protect radical intermediates from off-pathway reactions.[19,20] The enzymes act as a scaffold to protect the generated radical species by shielding it from solvent and by providing a framework to prevent the radical intermediate from moving great distances by either tightly binding the intermediate or positioning the necessary reacting partners within van der Waals (VDW) distances of each other, favoring on-pathway reactions.

6-CP is an oxidized analogue of the QueE substrate. The structure of 6-CP complexed with *Bm*QueE revealed that the 5′-carbon of the deoxyadenosine moiety of SAM is 3.2 Å away from one of the carboxylate oxygen atoms and 4.9 Å away from the sp^2 hybridized C-6 of 6-CP (Figure 1C). This close proximity between the substrate analogue and cofactor suggests

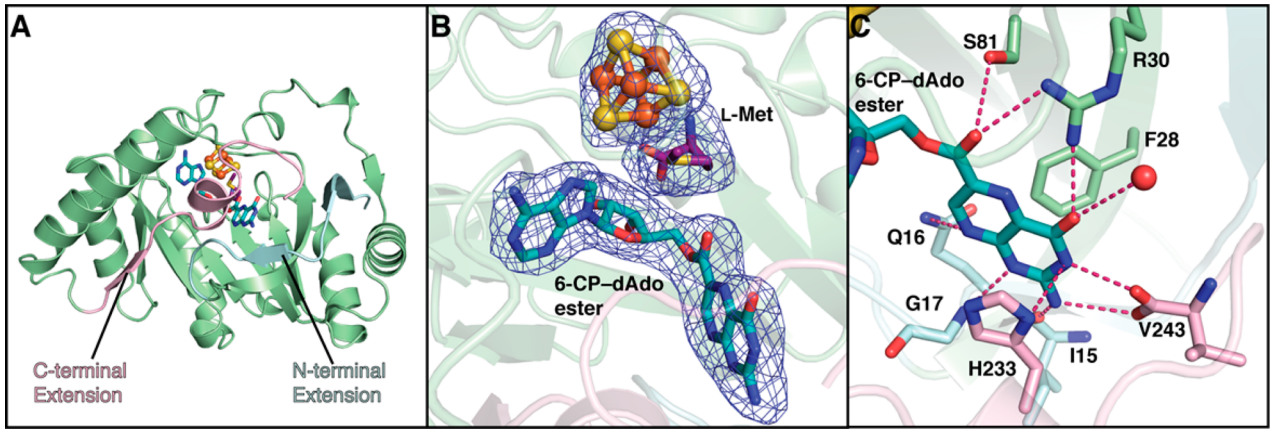

Figure 2. Adduct bound structure of *Bs*QueE. (A) The monomeric subunit of dimeric *Bs*QueE is composed of a central partial TIM domain (green) with N-terminal (light blue) and C-terminal (pink) extensions. The adduct and L-methionine carbons are colored teal and purple, respectively. The iron and sulfur atoms of the cluster are colored orange and yellow, respectively. (B) Simulated annealing omit density maps for the SAM radical [4Fe4S] cluster, L-methionine (colored purple) and the adduct refined as 6-CP−dAdo ester (teal), contoured at 3σ. (C) Interactions between the 6-CP moiety of 6-CP−dAdo ester (teal) and protein residues. Regions of protein colored as in (A) and atoms colored as described in Figure 1B.

DOI: 10.1021/jacs.6b11381
J. Am. Chem. Soc. 2017, 139, 1912−1920

that the enzyme may instead catalyze a group transfer reaction in cases where an H atom is not present.

In our continuing structure/function studies of QueE, we made a serendipitous discovery in the structure of the *Bacillus subtilis* QueE (*Bs*QueE) homologue crystallized in the presence of SAM and 6-CP. The electron density in the active site did not resemble that of 6-CP, but rather, the substrate analogue appeared to have undergone a modification that involved attachment to the 5′-dAdo of SAM. Therefore, we initiated studies to determine if 6-CP is an alternative substrate. Herein, we show that 6-CP is indeed a substrate for the QueE homologues from both *B. subtilis* and *B. multivorans*. However, unlike the H atom abstraction catalyzed with CPH_4, 6-CP undergoes two distinct catalytic outcomes. One of these leverages the ability of the enzyme to bind and reductively cleave SAM, but instead of H atom abstraction, a radical addition is performed. In the other, by contrast, QueE binds SAM and facilitates group transfer in the absence of dithionite to form the 6-carboxypterin-5′-deoxyadenosyl (6-CP−dAdo) ester covalent adduct observed in the crystal structure. These findings have implications in the functional role of uncharacterized enzymes in the radical SAM superfamily.

RESULTS

X-ray Structure of *Bs*QueE with a 6-CP−dAdo Ester Covalent Adduct. An initial X-ray crystal structure of dimeric His_6 tagged *Bs*QueE was determined to 2.55 Å resolution by Multiwavelength Anomalous Dispersion (MAD) phasing, which was then used to phase a 2.4 Å resolution structure of dimeric *Bs*QueE that contains a 6-CP−dAdo ester covalent adduct (Figure 2, Table S1). Similar to the *Bm*QueE structure, the monomeric subunit of *Bs*QueE is composed of a partial $(\beta/\alpha)_6$ TIM barrel fold, which is characteristic of radical SAM enzymes.[17,18] The active site is located within the lateral opening of the partial barrel (Figure 2A), and is flanked by N- and C- terminal regions, the latter of which protects the active site from solvent.

Although we crystallized *Bs*QueE with SAM and 6-CP, the electron density was not consistent with intact versions of these two molecules being bound in the active site. When an intact SAM was refined, negative difference density appeared for the C5′-S bond of SAM, suggesting that SAM has undergone cleavage to form methionine and 5′-dAdo (Figure 3A).

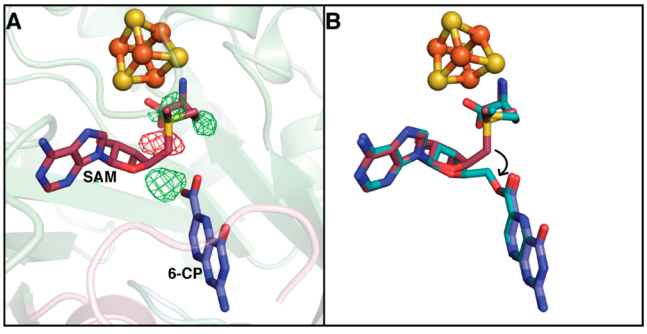

Figure 3. Formation of the *Bs*QueE adduct species. (A) Difference electron density maps obtained when refining data with intact SAM (maroon) and 6-CP (slate). Positive and negative difference densities are displayed as green and red meshes, respectively, contoured at 3σ. The iron−sulfur cluster is in orange and yellow. (B) In order to form the adduct (teal), the ribose ring of 5′-dAdo must rotate about 30° from its initial position in SAM.

Additionally, positive difference density appeared between the C5′ position of SAM and a carboxylate oxygen of 6-CP, indicating that a new ester bond may have been formed between these two molecules, requiring a rotation of about 30° around the ribose to bring the 5′-dAdo moiety toward 6-CP (Figure 3B). The resulting adduct can be described as a 5′-deoxyadenosyl ester of 6-CP (6-CP−dAdo ester) and is an excellent fit to omit map density (Figure 2B). Methionine, the other cleavage product of SAM, is also observed bound as expected for a SAM radical protein, i.e., coordinating the unique iron of the [4Fe-4S] cluster through its α-carboxyl and α-amino groups (Figure 2B).

The newly formed 6-CP−dAdo ester adduct spans the SAM and 6-CP binding sites on *Bs*QueE with the adenine and pterin rings residing in nearly perpendicular planes relative to one another (Figure 2B). The enzyme employs known SAM binding motifs for interactions with the 5′-dAdo moiety of the newly formed adduct (Figure 4),[21] and despite the 30° rotation of the 5′-dAdo about the ribose required to form the adduct, the interactions between the ribose and the protein are maintained (Figure 4). The planar pterin ring of the 6-CP moiety of the adduct is also bound similarly to how 6-CP was bound in the *Bm*QueE·6-CP·SAM structure.[15] It is positioned in the active site by a number of $\pi-\pi$ and electrostatic interactions from residues located in the protein core and the N- and C-terminal extensions (Figure 2C). The pterin ring moiety of the 6-CP−dAdo ester adduct stacks with the Phe28 and His233 residues from the N- and C-terminal extensions and is further held in place by various hydrogen bonds, including hydrogen bonds to the N3 and exocyclic amine by the carboxyl group of the C-terminal residue, Val243. One new hydrogen bond between the protein residue Gln16 and the pterin ring, positioning N8 of the pterin, was identified in this structure containing the covalent adduct (Figure 2C). Although this glutamine residue is conserved in *Bm*QueE, it is not in the proper orientation or within sufficient distance (5.9 Å from N8 of the pterin) to interact with 6-CP in that structure.[15] Instead, a water molecule is observed to bridge an interaction between this glutamine and the pterin N8 atom.

The mechanism by which 6-CP−dAdo ester forms in the active site of QueE cannot be gleaned from the structures alone. Although it has not been demonstrated that cluster reduction by the X-ray beam can lead to the reductive cleavage of SAM, it has not been ruled out either. In this scenario, formation of the 6-CP adduct could occur by a radical addition route. However, it is also possible that the close juxtaposition of SAM to 6-CP when both are bound to the enzyme could allow for the carboxylate oxygen of 6-CP to attack the 5′-position of the deoxyadenosine, displacing methionine to form the 6-CP−dAdo ester adduct.

6-CP Is an Alternative Substrate for QueE. To probe whether the 6-CP−dAdo ester observed in the crystal structure could have arisen from a reaction related to the radical-mediated ring contraction observed with CPH_4, we set up assays with 6-CP in the presence of SAM and *Bs*QueE under reducing conditions using dithionite. The reactions were quenched with acid and analyzed via LC−MS. A new product was observed to elute at ca. 39 min when *Bs*QueE, 6-CP, and SAM were present in the reaction. The appearance of this new product was dependent on the presence of enzyme, 6-CP, and SAM (Figure 5A). The rate of formation of this species, measured in a separate experiment, is ~0.0013 ± 0.0002 min^{-1},

DOI: 10.1021/jacs.6b11381
J. Am. Chem. Soc. 2017, 139, 1912−1920

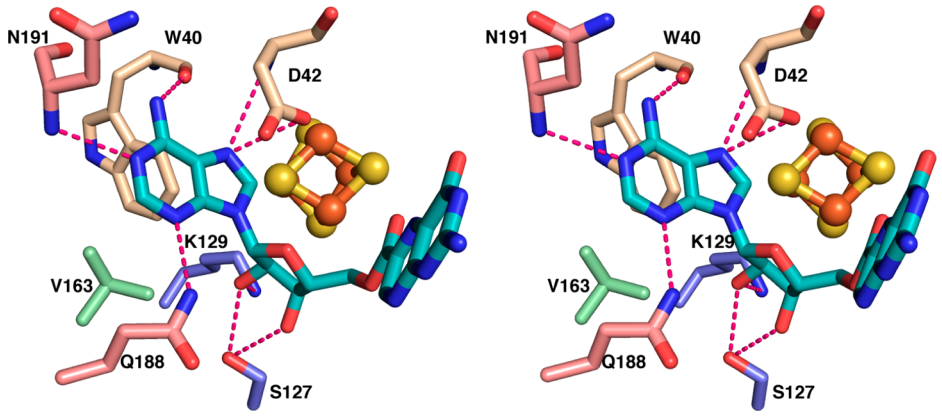

Figure 4. Walleyed stereoview of the binding interactions of *Bs*QueE with the 5′-dAdo moiety of the adduct species. The 5′-dAdo moiety binds to *Bs*QueE using previously characterized SAM binding motifs; residues of the ribose motif (slate) interact with the hydroxyl groups of the ribose ring through the hydroxyl and amino groups of Ser127 and Lys129 respectively, the β5 or GXIXGXXE motif (green) provides hydrophobic interactions to the adenine ring, and the β6 motif (salmon) provides interaction to the nitrogen atoms of the adenine ring positioning it in the active site via hydrogen bonds from the amide of Gln188 and the backbone amide of Asn191. Two residues from the cluster binding loop (tan) provide both $\pi-\pi$ interactions as well as hydrogen bonds to assist in the orientation of the adenine ring in the active site.

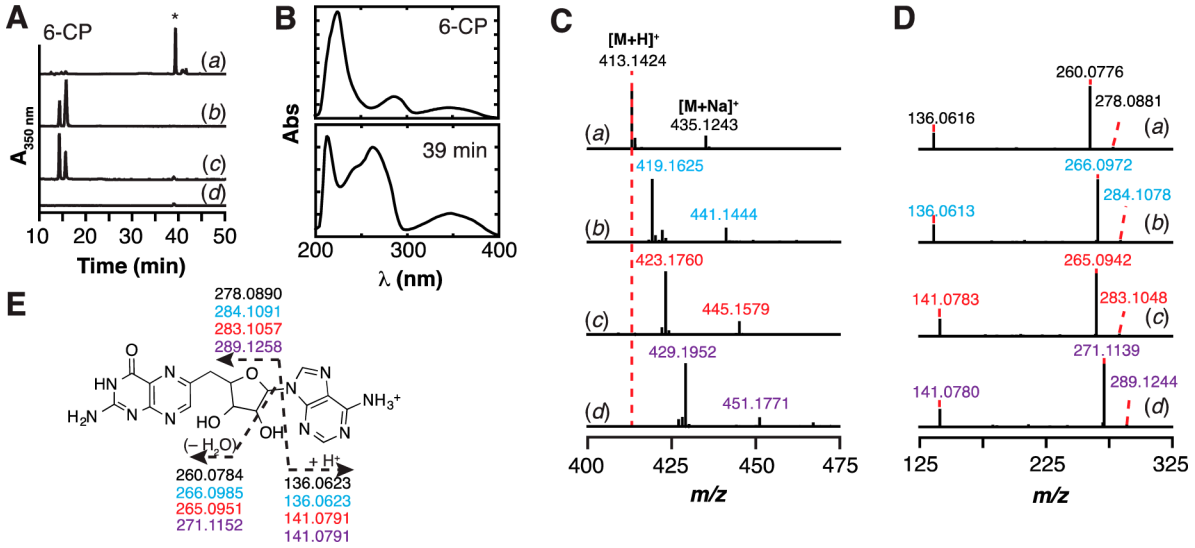

Figure 5. QueE catalyzes the conversion of 6-CP to a new pterin-containing species in the presence of dithionite and SAM. (A) HPLC chromatogram of reactions monitored at 350 nm showing that QueE can turnover 6-CP in the presence of SAM to a new product (*) with retention time of 39 min (*a*). This peak was not observed in the control reactions where either *Bs*QueE (*b*), SAM (*c*), or 6-CP (*d*) were omitted. 6-CP elutes at 15 min under these conditions. (B) The UV−visible spectra of 6-CP and the new product eluting at ca. 15 and 39 min, respectively. (C) Mass spectra of product eluting at 39 min isolated from reaction of *Bs*QueE under reducing conditions with natural abundance 6-CP and natural abundance SAM (black) (*a*); [U−$^{13}C_7$] 6-CP and natural abundance SAM (blue) (*b*); natural abundance 6-CP and [$^{13}C_{10}$-dAdo]-SAM (red) (*c*); or [U−$^{13}C_7$]-6-CP and [$^{13}C_{10}$-dAdo]-SAM (purple) (*d*). The species that is +22 amu relative to the $[M + H]^+$ corresponds to $[M + Na]^+$. (D) HCD fragmentation analysis of the 6-CP adduct formed under reducing conditions with natural abundance 6-CP and natural abundance SAM (black) (*a*); [U−$^{13}C_7$] 6-CP and natural abundance SAM (blue) (*b*); natural abundance 6-CP and [$^{13}C_{10}$-dAdo]-SAM (red) (*c*); or [U−$^{13}C_7$]-6-CP and [$^{13}C_{10}$-dAdo]-SAM (purple) (*d*). (E) The fragmentation patterns in (D) allow assignment of the new species at 39 min to 6-dAP.

which is 150-fold slower than that for formation of CDG from CPH_4.

Inspection of the UV−visible-spectrum of the new product eluting at 39 min revealed features at 350 nm reminiscent of 6-CP, as well as a substantial peak at 260 nm (Figure 5B). The simplest explanation for this observation is the presence of adenine originating from SAM, since the formation of this product is SAM dependent (Figure 5Ac). Therefore, we examined if the new product represents a covalent adduct between 5′-dAdo and 6-CP by mass spectrometry. The theoretical m/z of such a product is expected to be 457.1333 ($[M + H]^+$). However, the mass spectrum of the new peak eluting at 39 min exhibits a m/z of 413.1424, which is 43.9909 amu lighter than a simple adduct between 6-CP and 5′-dAdo (Figure 5Ca). The loss of CO_2 (43.9898 amu) from a 5′-dAdo-6-CP covalent adduct would yield a m/z of 413.1435, which is within 2.7 ppm of the observed mass.

The identity of the new product was explored using isotopically enriched SAM and 6-CP. SAM was synthesized enzymatically from unlabeled methionine and [U−$^{13}C_{10}$] ATP to label the 10 carbons in 5′-dAdo moiety of SAM. [U−$^{13}C_7$] 6-CP was synthesized by permanganate oxidation of [U−$^{13}C_7$] CPH_4, which itself was obtained by the successive actions of GTP cyclohydrolase I and CPH_4 synthase on [U−$^{13}C_{10}$] GTP.

DOI: 10.1021/jacs.6b11381
J. Am. Chem. Soc. 2017, 139, 1912−1920

Mass spectrometry revealed the [$^{13}C_{10}$] SAM and [U−$^{13}C_7$] 6-CP to be >87% and >95% enriched, respectively (Figure S2 and S3). Isotopically enriched SAM and 6-CP analogues were incubated with QueE and the mass spectra of the resulting products were compared to reactions containing natural abundance 6-CP and natural abundance SAM (Figure 5C). When 6-CP is substituted with [U−$^{13}C_7$] 6-CP, the m/z for the resulting product shifts from 413.1424 to 419.1625, consistent with the retention of six of the seven possible ^{13}C enriched carbons from 6-CP (theoretical m/z 419.1636, 2.6 ppm error) (Figure 5Cb). By contrast, with [$^{13}C_{10}$-dAdo] SAM the m/z shifts from 413.1424 to 423.1760 (Figure 5Cc). The observed 10 amu shift (theoretical m/z 423.1770, 2.4 ppm error) indicates that 5′-dAdo from SAM is incorporated in the new product. This finding is consistent with the increase at 260 nm for the product (Figure 5B). When both [$^{13}C_{10}$]-SAM and [U−$^{13}C_7$]-6-CP are incubated with QueE, the mass shifts by 16 amu from m/z 413.1424 to 429.1952 (theoretical m/z of 429.1971, 4.4 ppm error) indicating that the new species was derived from both 6-CP (minus one carbon) *and* the 5′-dAdo moiety of SAM (Figure 5Cd).

Mass spectral fragmentation of the products from the reaction mixtures with natural abundance and isotopically enriched substrates were carried out to further probe the structure of the adduct. Three fragments are observed by MS/MS of the product ([M + H]$^+$ m/z of 413.1424) in reactions containing natural abundance SAM and 6-CP, which are consistent with adenine (m/z: observed, 136.0616; theoretical, 136.0623), dehydrated decarboxylated pterin-ribose (m/z: observed, 260.0776; theoretical, 260.0784), and decarboxylated pterin-ribose (m/z: observed, 278.0881; theoretical, 278.0890) (see Figure 5Da and 5E). MS/MS analysis of the corresponding [M + H]$^+$ peaks in reactions containing isotopically enriched substrates exhibited the expected isotopic shifts and were readily assigned to the fragments observed with the natural abundance substrate, with exception of expected isotopic enrichment due to incorporation of ^{13}C from 6-CP (Figure 5Db), SAM (Figure 5Dc), or both (Figure 5Dd). The fragmentation patterns observed with the isotopically enriched product are readily mapped onto that obtained with the natural abundance product. These data are consistent with the new product being 6-deoxyadenosylpterin (6-dAP) (Figure 5E). However, this product is not consistent with the adduct observed in the structure of *Bs*QueE solved in the presence of SAM and 6-CP.

QueE Catalyzes Two Different 6-CP Reactions Depending on the Presence of Reductant. Formation of 6-dAP requires incubating *Bs*QueE, SAM, and 6-CP in the presence of dithionite. As a control, to determine if the product with m/z of 413.1424 was dependent on the presence of reductant, *Bs*QueE was incubated with 6-CP in the *absence* of dithionite. Surprisingly, a new peak appeared at ca. 42 min in the chromatogram of the reaction where only dithionite was omitted (Figure 6b), which is distinct from the peak at 39 min observed in the presence of dithionite (Figure 6d). As with the species at 39 min, the appearance of the 42 min species requires the presence of *Bs*QueE (Figure 6a and 6c). The formation of this new species requires *Bs*QueE, SAM, and 6-CP (Figure 7Aa), and it is not observed when any of these components are omitted (Figure 7Ac−e). As with the 6-dAP product, this new product exhibits UV−visible spectral features consistent with both 6-CP and adenine, but its retention time of 42 min is significantly different suggesting that it is not 6-dAP (Figure 7B). The rate of formation of this product ($5.6 \pm 0.9 \times 10^{-5}$ min^{-1}) is 23- and 3600-fold slower than formation of 6-dAP and CDG, respectively. Although the strong reductant dithionite was omitted from these reactions, they were carried out under reducing conditions in the presence of 10 mM DTT in an anaerobic chamber. Control experiments, however, show that the new product at 42 min is observed even in the absence of DTT (Figure 7Ab).

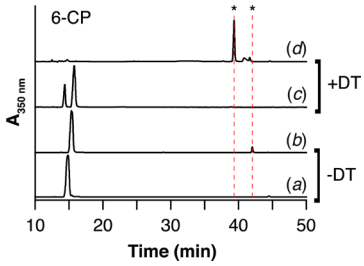

Figure 6. HPLC chromatogram of *Bs*QueE reactions containing SAM and 6-CP monitored at 350 nm. In the absence of dithionite, a new peak was observed that elutes at 42 min (*b*) instead of the peak that elutes at 39 min (*d*) that was observed in the presence of dithionite. Both the 39 and 42 min peaks require *Bs*QueE (*c* and *a*, respectively).

We examined the identity of the new product via mass spectrometry. The species that elutes at ca. 42 min exhibits a m/z of 457.1320 ([M + H]$^+$) (Figure 7Ca). This new product is most consistent with the 6-CP−dAdo ester adduct (theoretical m/z = 457.1333) observed in the crystal structure. The identity of the product was further probed with natural abundance and ^{13}C enriched SAM and 6-CP. In contrast to 6-dAP, when the reactions were carried out in the absence of dithionite with [U−$^{13}C_7$] 6-CP the mass of the 42 min peak shifts from 457.1320 to 464.1560 (theoretical m/z 464.1567, 1.5 ppm error) (Figure 7Cb), which is consistent with retention of all the carbons of 6-CP. Replacing natural abundance SAM with [$^{13}C_{10}$-dAdo] SAM results in a 10 amu shift in the m/z for [M + H]$^+$ from 457.1320 to 467.1654 (theoretical m/z 467.1668, 3.0 ppm error) (Figure 7Cc). Finally, when both isotopically enriched substrates are incubated with *Bs*QueE the [M + H]$^+$ mass shifts by 17 amu from m/z 457.1320 to 474.1906 (theoretical m/z 474.1902, 0.8 ppm error) (Figure 7Cd).

To probe the structure of the new product, the [M + H]$^+$ peak from each reaction mixture was subjected to MS/MS fragmentation. The fragmentation spectrum obtained from the natural abundance product is shown in Figure 7Da. The observed fragments are consistent with adenine (m/z: observed, 136.0614; theoretical, 136.0623), 6-CP (m/z: observed, 208.0461; theoretical, 208.0471), dehydrated 6-CP-ribose (m/z: observed, 304.0669; theoretical, 304.0682), 6-CP-ribose (m/z: observed, 322.0774; theoretical, 322.0788), 6-CP-deoxyadenosine that has lost the equivalent of two water molecules (m/z: observed, 421.1106; theoretical, 421.1122), and dehydrated 6-CP-deoxyadenosine (m/z: observed, 439.1211; theoretical, 439.1227) (Figure 7Da and 7E). MS/MS spectra of the corresponding [M + H]$^+$ peaks in reactions containing isotopically enriched substrates exhibit the expected isotopic shifts and are readily assigned to the fragments observed with the natural abundance substrate, with exception of expected isotopic enrichment due to incorporation of ^{13}C from 6-CP (Figure 7Db), SAM (Figure 7Dc), or both (Figure 7Dd). The fragmentation patterns observed with the isotopically enriched product are readily mapped onto that obtained

DOI: 10.1021/jacs.6b11381
J. Am. Chem. Soc. 2017, 139, 1912−1920

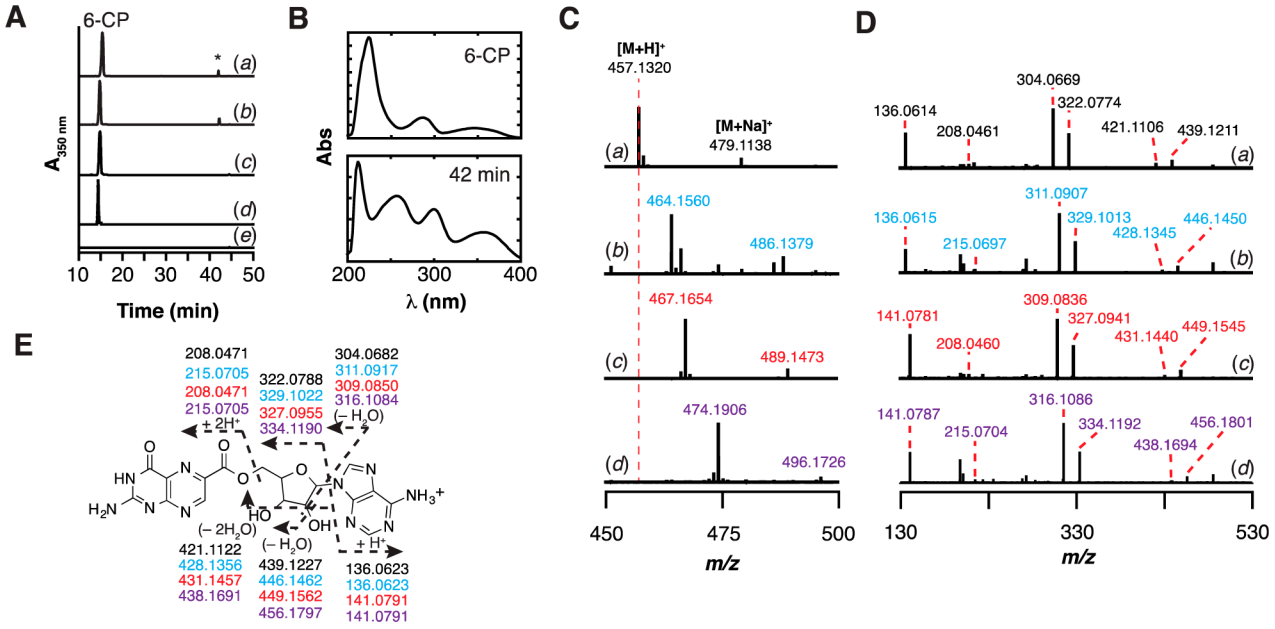

Figure 7. Conversion of 6-CP to 6-CP−dAdo ester under nonreducing conditions. (A) HPLC chromatogram monitored at 350 nm of reactions showing that *Bs*QueE can turnover 6-CP in the presence of SAM to a new product denoted by * (*a*). To rule out that DTT, which was present in the reaction was not responsible, the reactions were repeated in the absence of DTT and the same result was obtained (*b*). However, this species was not observed in the control reactions where either *Bs*QueE (*c*), SAM (*d*), or 6-CP (*e*) were omitted. (B) The UV−visible spectra of 6-CP and the new product, eluting at 15 and 42 min, respectively, show that the new species has spectral features of 6-CP and an additional feature ∼260 nm. (C) Mass spectra of product (eluting at ca. 42 min) isolated from reactions of *Bs*QueE in the absence of dithionite with natural abundance 6-CP and natural abundance SAM (black) (*a*); [U−$^{13}C_7$]-6-CP and natural abundance SAM (blue) (*b*); natural abundance 6-CP and [$^{13}C_{10}$-dAdo]-SAM (red) (*c*); or [U−$^{13}C_7$]-6-CP and [$^{13}C_{10}$-dAdo]-SAM (purple) (*d*). The species at +22 amu relative to the $[M + H]^+$ corresponds to $[M + Na]^+$. (D) CID fragmentation analysis of the new reaction product obtained with natural abundance 6-CP and natural abundance SAM (black) (*a*); [U−$^{13}C_7$] 6-CP and natural abundance SAM (blue) (*b*); natural abundance 6-CP and [$^{13}C_{10}$-dAdo]-SAM (red) (*c*); or [U−$^{13}C_7$]-6-CP and [$^{13}C_{10}$-dAdo]-SAM (purple) (*d*). (E) The fragmentation patterns in (D) allow assignment of the new species at 42 min to 6-CP−dAdo ester.

with the natural abundance product, further confirming the structural assignment of 6-CP−dAdo ester (Figure 7E). Therefore, the product observed in the aforementioned *Bs*QueE crystal structure forms in the absence of reductant by taking advantage of the inherent reactivity of SAM toward nucleophilic attack.

Mg^{2+} Dependence of Alternative Activities. Previous structural and functional investigations of *Bs*QueE and *Bm*QueE revealed an unexpected requirement for Mg^{2+} in the conversion of CPH_4 to CDG. Structures of *Bm*QueE complexed with substrate (CPH_4) and product (CDG) show that the Mg^{2+} provides key contacts with the substrate and product, thus anchoring the molecules in the active site. Interestingly, $Mg^{2+}$is not observed in the *Bs*QueE structure of the 6-CP−dAdo ester adduct described above and the *Bm*QueE complexed with 6-CP.[15] Therefore, we sought to determine if the divalent cation was required for the formation of either 6-dAP or 6-CP−dAdo ester. We observed no significant change in the rates of formation for 6-dAP or 6-CP-dAdo ester when Mg^{2+} was omitted from the reaction or when it was added to a final concentration of 2 mM. However, it is possible that Mg^{2+} was present in the reaction mixture as a contaminant from the purified protein, SAM, or 6-CP. Therefore, we subjected an aliquot of each reaction mixture to ICP-MS to analyze for the presence of Mg^{2+}. The concentration of Mg^{2+} in each reaction mixture was not detectable above the ∼1 μM background in the trace-metals grade nitric acid used to prepare the sample. This shows that unlike the wild-type function of QueE, the formation of either 6−CP product is not enhanced by the presence of Mg^{2+}.

***B. multivorans* QueE Catalyzes the Formation of Both 6-dAP and 6-CP−dAdo Ester.** The structural investigation of *B. multivorans* QueE revealed that this homologue was capable of binding 6-CP in the active site in a similar fashion to that of the *B. subtilis* QueE.[15] The two homologues share 21% sequence identity and 31% sequence similarity. Therefore, we sought to determine if 6-CP was an alternative substrate for the QueE homologue from *B. multivorans* to determine if the divergent outcomes of turnover with 6-CP in the presence or absence of reductant is an intrinsic property of the enzyme and not specific to the *B. subtilis* protein. Indeed, when *Bm*QueE was incubated with 6-CP in the presence of reductant, a new product was observed in the extracted ion chromatogram (Figure 8A). Based on both the retention time (ca. 37 min) and MS data (*m*/*z* of 413.1425) the species is 6-dAP (Figure 8B).

In parallel to the *Bs*QueE, in the absence of reductant, we observe a peak in the extracted ion chromatogram of the reaction at 42 min (Figure 8Ca), which requires the enzyme (Figure 8Cb). The *m*/*z* of the species eluting at 42 min, 457.1322, is identical to 6-CP-dAdo ester (Figure 8D). Therefore, both *Bs*QueE and *Bm*QueE catalyze identical polar and radical mediated transformations utilizing 6-CP as an alternate substrate.

DISCUSSION

Since the unification of the radical SAM superfamily in 2001, the number of members has expanded from ∼600 to >113 000.[2,11] All members of the radical SAM superfamily characterized to date have been shown to utilize a [4Fe-4S] cluster, which is typically coordinated by the CxxxCxxC motif,

DOI: 10.1021/jacs.6b11381
J. Am. Chem. Soc. 2017, 139, 1912−1920

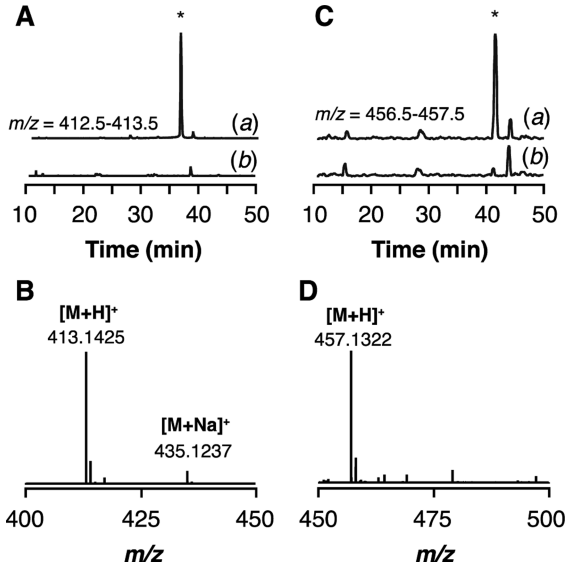

Figure 8. *B. multivorans* QueE catalyzes the formation of 6-dAP and 6-CP−dAdo ester in the presence or absence of reductant, respectively. (A) LC−MS extracted ion chromatograms monitoring at *m*/*z* 412.5−413.5 of reactions containing natural abundance 6-CP and natural abundance SAM incubated with (*a*) or without (*b*) *Bm*QueE in the presence of reductant. (B) Mass spectra of product eluting at ca. 37 min isolated from reaction of *Bm*QueE under reducing conditions with natural abundance 6-CP and natural abundance SAM. (C) LC−MS extracted ion chromatograms monitoring at *m*/*z* 456.5−457.5 of reactions containing natural abundance 6-CP and natural abundance SAM incubated with (*a*) or without (*b*) *Bm*QueE in the absence of reductant. (D) Mass spectra of product eluting at ca. 42 min isolated from reaction of *Bm*QueE with natural abundance 6-CP and natural abundance SAM in the absence of reductant.

to mediate the reductive cleavage of SAM commonly affording the dAdo· (Figure 1A). The dAdo· abstracts a H atom from substrate to initiate a myriad of radical-mediated transformations.[1]

While under some conditions, alternate reactivity with substrate analogues have been noted leading to novel products,[22−25] to date, with two notable exceptions, SAM participates by radical mechanism. Two members of the superfamily (RlmN and Cfr) are unique in that they utilized SAM for *both* polar and radical transformations.[6,7] The homologous enzymes RlmN and Cfr catalyze the methylation of C-2 or C-8 of the adenine ring of A_{2503} in 23S rRNA. Similarly, TsrM catalyzes the methylation of tryptophan in an as yet undetermined mechanism that does not appear to entail reductive cleavage of SAM.[8−10] The structure of RlmN reveals that as with other radical SAM enzymes it adopts the partial TIM barrel $(\beta/\alpha)_6$ fold and the three cysteine thiolates of the CxxxCxxC motif coordinate three iron atoms of a catalytically essential [4Fe-4S] cluster.[26] The fourth iron of the cluster is coordinated by the α-amino and α-carboxylate moieties of SAM. Functionally, both RlmN and Cfr reductively cleave SAM, as expected for a radical SAM superfamily. However, what sets these two enzymes apart from the rest of the superfamily is that they catalyze methyl transfer from SAM coordinated to the [4Fe-4S] cluster to an active site Cys residue using a polar substitution mechanism, in addition to reductively cleaving a second equivalent of SAM at the [4Fe-4S] cluster to mediate the methyl transfer from the methyl-Cys to the A_{2503}.[6,7] RlmN and Cfr are examples of radical SAM enzymes that use SAM in both a polar and radical capacity in the same catalytic cycle.

The involvement of SAM in polar group transfer is a common reaction that occurs in a variety of biological processes including gene regulation and metabolite biosynthesis. However, enzymes that utilize SAM exclusively as a methyl donor are structurally distinct from the radical SAM superfamily, adopting an $\alpha\beta\alpha$-sandwich fold that is reminiscent of the Rossmann fold.[27]

The physiological role of QueE is to harness dAdo· from reductively cleaved SAM to catalyze the radical mediated ring rearrangement in the conversion of CPH_4 to CDG.[14] This enzyme has been extensively characterized both structurally and functionally.[14−16] Structures of *Bm*QueE show that the enzyme is able to bind an oxidized analogue of the substrate, 6-CP, in a manner similar to that of the substrate (CPH_4) and product (CDG) (Figure S1).[15] We initiated the biochemical studies in this paper when we observed an unusual product, 6-CP−dAdo ester, in the X-ray crystal structure of *Bs*QueE·6-CP·SAM complex. We are able to produce the 6-CP−dAdo ester in vitro when QueE is incubated with 6-CP and SAM in the absence of dithionite. Under reducing conditions, an alternate product, 6-dAP was observed and characterized. This product is analogous to that observed for the radical SAM enzymes, MqnE, in the futalosine biosynthetic pathway, and HydE, in the assembly of the [FeFe]-hydrogenase active site.[28,29] Additionally, Knappe and co-workers observed that pyruvate formate-lyase-activating enzymes catalyzed a similar addition of dAdo· to the olefinic β carbon of a dehydroalanine residue in a dehydroalanine-containing octapeptide.[30]

In the presence of the strong reductant dithionite, QueE generates the dAdo·, which subsequently reacts with 6-CP via a radical addition reaction leading to the decarboxylation of 6-CP and the formation of 6-dAP (Scheme 1, right). Although 6-CP is not the natural substrate, this reaction is not surprising as the current understanding of radical SAM enzymes is that they generate radical intermediates and stabilize them by providing scaffolds that minimize off-pathway reactions.[19,20] One

Scheme 1. Proposed Mechanisms of the Polar (Left) And Radical Addition (Right) Reactions to Form 6-CP−dAdo Ester and 6-dAP, Respectively

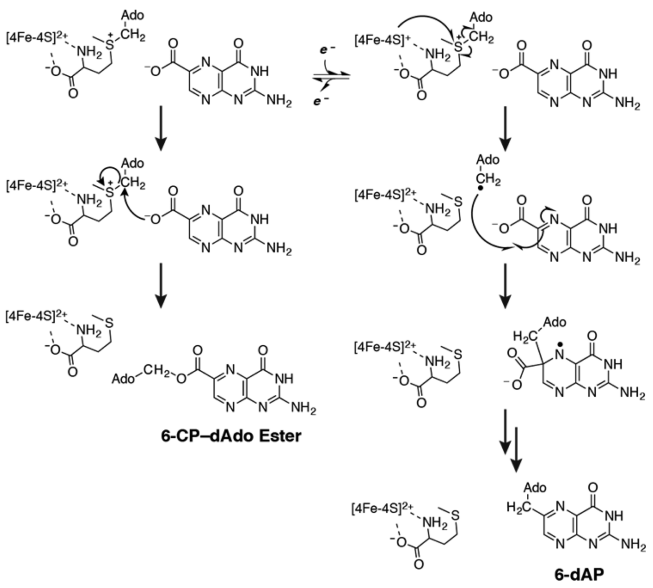

DOI: 10.1021/jacs.6b11381
J. Am. Chem. Soc. 2017, 139, 1912−1920

mechanism to favor on-pathway reactions is to properly orient the substrate within VDW distances of the dAdo·.

6-CP was modified by SAM in the absence of reductant, but instead of a radical addition, we observed formation of an ester linkage between 6-CP and the 5′-deoxyadenosine moiety of SAM. To explain this, we propose a polar substitution mechanism (Scheme 1, left) analogous to that observed in methyltransferases and the radical SAM enzymes RlmN and Cfr.[6,7] Close inspection of the *Bm*QueE structure with 6-CP bound shows that one of the carboxylate oxygen atoms is only 3.2 Å from the C5′ of SAM, where it could participate in nucleophilic substitution (Figure 1C). The *Bs*QueE structure further shows that a carboxylate oxygen is within 2.9 Å of R30, a conserved residue capable of stabilizing the deprotonated form of the 6-CP carboxylate and potentially activating it for nucleophilic attack on C5′ of SAM (Figure 2C). The resulting adduct characterized in this study provides evidence of now a third radical SAM enzyme that is capable of using SAM coordinated to a [4Fe-4S] cluster for polar group transfer. However, what sets this apart from RlmN and Cfr is the fact that 6-CP is not a natural substrate for QueE, therefore the formation of 6-CP−dAdo ester and 6-dAP are promiscuous activities for this radical SAM enzyme. Unlike the radical mediated ring contraction reaction of CPH_4 to form CDG, the polar and radical additions of 5′-dAdo to 6-CP do not appear to require magnesium. This finding may suggest that magnesium is involved in minimizing off-pathway reactivity with the substrate. Certainly, the binding of the carboxylate of CPH_4 to the magnesium may block formation of the ester adduct. Additional studies with alternate substrate analogues should aid in delineating the role(s) of the active site residues and the magnesium ion in directing the promiscuous activities of QueE.

The current work in the radical SAM superfamily has provided overwhelming evidence that these enzymes use the SAM bound [4Fe-4S] cluster to reductively cleave SAM to initiate radical-mediated reactions.[1] However, the recent observations of RlmN, Cfr, and now QueE utilizing the same fold to catalyze polar group transfer from SAM questions the paradigm that *all* proteins containing the CxxxCxxC motif reductively cleave SAM.[6,7] The sulfonium of SAM activates it to transfer 5′-dAdo, methyl, or 3-amino-3-carboxypropyl moieties to any properly positioned acceptor molecule by nucleophilic displacement. Booker and colleagues have provided a beautiful example of polar methyl group transfer by a cluster-bound SAM.[6,7,26] The studies presented here are the first to demonstrate the polar transfer of 5′-dAdo. Our prediction is that as more presumed radical SAM enzymes are studied, that additional polar group transfer from SAM will be discovered.

CONCLUSION

The original report by Sofia and co-workers nearly 20 years ago where the radical SAM superfamily was identified by the presence of the CxxxCxxC motif occurred before the explosion of genome sequences.[2] Moreover, in the intervening decades, studies from several laboratories have uncovered a surprising range of reactivity.[1] The studies on polar methyl group transfer in RlmN and Cfr,[6,7] the methylation catalyzed by TsrM,[8−10] and this manuscript show that, at least in principle, moieties attached to the sulfonium of SAM can be transferred by a polar route in radical SAM enzymes. To be sure, the formation of 6-CP−dAdo ester is a promiscuous activity in a protein that is designed to do an entirely different type of transformation. However, it is now generally accepted that new activities emerge in enzymes by optimization of low-level reactions. We propose that with >113 000 annotated radical SAM enzymes that it is only a matter of time before additional enzymes whose sole function is not methyl group transfer or radical chemistry will emerge.

ASSOCIATED CONTENT

Supporting Information

The Supporting Information is available free of charge on the ACS Publications website at DOI: 10.1021/jacs.6b11381.

Figures S1−S3; Table S1; Experimental Procedures (PDF)

AUTHOR INFORMATION

Corresponding Author

*vahe@chem.utah.edu

ORCID

Nathan A. Bruender: 0000-0002-6129-8897

Vahe Bandarian: 0000-0003-2302-0277

Present Addresses

[¶]Department of Chemistry and Biochemistry, St. Cloud State University, 720 Fourth Avenue S., St. Cloud, Minnesota 56301, United States.

[▽]Department of Chemistry, University of Massachusetts−Boston, 100 Morrissey Blvd., Boston, Massachusetts 02125, United States.

Notes

The authors declare no competing financial interest.

[#]Dr. McCarty initiated in the 6-CP studies while a graduate student at the University of Arizona under the direction of V.B. He passed away unexpectedly in 2014.

ACKNOWLEDGMENTS

This work is based upon research conducted at the Northeastern Collaborative Access Team beamlines, which are funded by the National Institute of General Medical Sciences from the National Institutes of Health (P41 GM103403). The Pilatus 6M detector on 24-ID-C beamline is funded by a NIH-ORIP HEI grant (S10 RR029205). This research used resources of the Advanced Photon Source, a U.S. Department of Energy (DOE) Office of Science User Facility operated for the DOE Office of Science by Argonne National Laboratory under Contract No. DE-AC02-06CH11357. This work is also based in part on research conducted at the Advanced Light Source, which is supported by the Director, Office of Science, Office of Basic Energy Sciences, of the US Department of Energy under Contract DE-AC02-05CH11231. The work reported in this publication was supported by National Institutes of General Medical Sciences of the National Institutes of Health grant R01 GM72623 (awarded to V.B.) and a National Science Foundation Graduate Research Fellowship under Grant No. 1122374 (awarded to T.A.J.G.). C.L.D. is a Howard Hughes Medical Institute Investigator. The content is solely the responsibility of the authors and does not necessarily represent the official views of the National Institutes of Health.

REFERENCES

(1) Broderick, J. B.; Duffus, B. R.; Duschene, K. S.; Shepard, E. M. *Chem. Rev.* **2014**, *114*, 4229.

(2) Sofia, H. J.; Chen, G.; Hetzler, B. G.; Reyes-Spindola, J. F.; Miller, N. E. *Nucleic Acids Res.* **2001**, *29*, 1097.

DOI: 10.1021/jacs.6b11381
J. Am. Chem. Soc. 2017, 139, 1912−1920

(3) Walsby, C. J.; Ortillo, D.; Broderick, W. E.; Broderick, J. B.; Hoffman, B. M. *J. Am. Chem. Soc.* **2002**, *124*, 11270.
(4) Chen, D.; Walsby, C.; Hoffman, B. M.; Frey, P. A. *J. Am. Chem. Soc.* **2003**, *125*, 11788.
(5) Zhang, Y.; Zhu, X.; Torelli, A. T.; Lee, M.; Dzikovski, B.; Koralewski, R. M.; Wang, E.; Freed, J.; Krebs, C.; Ealick, S. E.; Lin, H. *Nature* **2010**, *465*, 891.
(6) Grove, T. L.; Benner, J. S.; Radle, M. I.; Ahlum, J. H.; Landgraf, B. J.; Krebs, C.; Booker, S. J. *Science* **2011**, *332*, 604−607.
(7) Grove, T. L.; Radle, M. I.; Krebs, C.; Booker, S. J. *J. Am. Chem. Soc.* **2011**, *133*, 19586.
(8) Pierre, S.; Guillot, A.; Benjdia, A.; Sandström, C.; Langella, P.; Berteau, O. *Nat. Chem. Biol.* **2012**, *8*, 957.
(9) Benjdia, A.; Pierre, S.; Gherasim, C.; Guillot, A.; Carmona, M.; Amara, P.; Banerjee, R.; Berteau, O. *Nat. Commun.* **2015**, *6*, 8377.
(10) Blaszczyk, A. J.; Silakov, A.; Zhang, B.; Maiocco, S. J.; Lanz, N. D.; Kelly, W. L.; Elliot, S. J.; Krebs, C.; Booker, S. J. *J. Am. Chem. Soc.* **2016**, *138*, 3416.
(11) Brown, S.; Babbitt, P. *Curr. Protoc. Bioinf.* **2014**, *48*, 2.10.1.
(12) McCarty, R. M.; Somogyi, A.; Lin, G.; Jacobsen, N. E.; Bandarian, V. *Biochemistry* **2009**, *48*, 3847.
(13) McCarty, R. M.; Bandarian, V. *Bioorg. Chem.* **2012**, *43*, 15−25.
(14) McCarty, R. M.; Krebs, C.; Bandarian, V. *Biochemistry* **2013**, *52*, 188.
(15) Dowling, D. P.; Bruender, N. A.; Young, A. P.; McCarty, R. M.; Bandarian, V.; Drennan, C. L. *Nat. Chem. Biol.* **2013**, *10*, 106.
(16) Bruender, N. A.; Young, A. P.; Bandarian, V. *Biochemistry* **2015**, *54*, 2903.
(17) Vey, J. L.; Drennan, C. L. *Chem. Rev.* **2011**, *111*, 2487.
(18) Dowling, D. P.; Vey, J. L.; Croft, A. K.; Drennan, C. L. *Biochim. Biophys. Acta, Proteins Proteomics* **2012**, *1824*, 1178.
(19) Lees, N. S.; Chen, D.; Walsby, C. J.; Behshad, E.; Frey, P. A.; Hoffman, B. M. *J. Am. Chem. Soc.* **2006**, *128*, 10145.
(20) Horitani, M.; Byer, A. S.; Shisler, K. A.; Chandra, T.; Broderick, J. B.; Hoffman, B. M. *J. Am. Chem. Soc.* **2015**, *137*, 7111.
(21) Nicolet, Y.; Drennan, C. L. *Nucleic Acids Res.* **2004**, *32*, 4015.
(22) Ji, X.; Li, Y.; Ding, W.; Zhang, Q. *Angew. Chem., Int. Ed.* **2015**, *54*, 9021.
(23) Bhandari, D. M.; Xu, H.; Nicolet, Y.; Fontecilla-Camps, J. C.; Begley, T. P. *Biochemistry* **2015**, *54*, 4767.
(24) Ji, X.; Li, Y.; Jia, Y.; Ding, W.; Zhang, Q. *Angew. Chem., Int. Ed.* **2016**, *55*, 3334.
(25) Ji, X.; Li, Y.; Xie, L.; Lu, H.; Ding, W.; Zhang, Q. *Angew. Chem., Int. Ed.* **2016**, *55*, 11845.
(26) Boal, A. K.; Grove, T. L.; McLaughlin, M. I.; Yennawar, N. H.; Booker, S. J.; Rosenzweig, A. C. *Science* **2011**, *332*, 1089.
(27) Martin, J. L.; McMillan, F. M. *Curr. Opin. Struct. Biol.* **2002**, *12*, 783.
(28) Mahanta, N.; Fedoseyenko, D.; Dairi, T.; Begley, T. P. *J. Am. Chem. Soc.* **2013**, *135*, 15318.
(29) Rohac, R.; Amara, P.; Benjida, A.; Martin, L.; Ruffie, P.; Favier, A.; Berteau, O.; Mouesca, J. M.; Fontecilla-Camps, J. C.; Nicolet, U. *Nat. Chem.* **2016**, *8*, 491.
(30) Volker Wagner, A. F.; Demand, J.; Schilling, G.; Pils, T.; Knappe, J. *Biochem. Biophys. Res. Commun.* **1999**, *254*, 306.

DOI: 10.1021/jacs.6b11381
J. Am. Chem. Soc. 2017, 139, 1912−1920